High-Resolution Carbon-13 Nuclear Magnetic Resonance Spectra and Structure of Amorphous and Crystalline Forms of Stereoregular Poly(methyl methacrylate)s[†]

J. Spěváček,* B. Schneider, and J. Straka

Institute of Macromolecular Chemistry, Czechoslovak Academy of Sciences, 162 06 Prague 6, Czechoslovakia

ABSTRACT: ^{13}C CP/MAS NMR spectra of amorphous and partly crystalline samples of isotactic (i) and syndiotactic (s) poly(methyl methacrylate) (PMMA), of a sample of partly crystalline stereocomplex PMMA, and ^{13}C MAS NMR spectra of a toluene gel of s-PMMA were measured. The observed two bands of α-CH$_3$ carbons in amorphous i-PMMA were assigned to trans and gauche backbone conformations; an effect of conformational structure on α-CH$_3$ carbon resonance was observed also with s-PMMA. High-resolution ^{13}C NMR spectra of the crystalline phase in i- and s-PMMA and stereocomplex PMMA were obtained from the experimental spectra by a computer difference technique; they differ from the spectra of amorphous samples by a splitting of some bands into two components and by differences in chemical shift values. These differences are interpreted by the existence of double-helix structures in crystalline forms of stereoregular PMMA. Also the observation of equal values of the proton spin–lattice relaxation time in rotating frame $T_{1\rho}{}^{H}$, for i- and s-components of stereocomplex PMMA is in agreement with this double-helix structure.

Introduction

The ability of stereoregular poly(methyl methacrylates) (PMMA) to form ordered aggregated structures in solution has been well documented.[1] Besides the aggregates of the so-called stereocomplex, generated by mixing of solutions of isotactic (i) and syndiotactic (s) PMMA, self-aggregation in solutions of only i-PMMA, or only s-PMMA, has also been described. At concentrations exceeding about 2%, stereocomplex or self-aggregate formation is manifested by the appearance of a gel. When the solvent is removed from such a system under conditions that do not disturb the stability of the aggregates, their structure remains preserved even in the solid state, and the resulting solid polymer is partly crystalline. Besides the partly crystalline solid stereocomplex PMMA,[1–3] the route via the aggregation state is also the only way to prepare semicrystalline s-PMMA either directly from a suitable solution[4,5] or by crystallization in the vapors of a solvent that promotes aggregation.[6,7] Semicrystalline i-PMMA can be prepared by prolonged annealing at elevated temperature;[3,8] without annealing it can be obtained by way of the gel stage from an o-xylene gel.[9] Relatively recent X-ray diffraction studies of crystalline i-PMMA have shown that its chains assume the form of a 10/1 double helix.[10,11] On the basis of X-ray diffraction measurements and conformational energy calculations, the structure of a double helix with a large number of units per turn has also been proposed for crystalline stereocomplex PMMA;[12] measurements of NMR and infrared (IR) spectra indicate that the structures of the crystalline state are already present in the aggregates of stereocomplex PMMA in solution.[5,13,14] The results of X-ray diffraction and IR spectroscopy indicate the presence of a helical conformation with a large number of units per turn both in aggregated and in crystalline s-PMMA.[5–7] Also in this case some evidence indicates the formation of structures of the double-helical type.[1,14–17] In all these helical structures, the conformational struc-

ture of the backbone chain is very near to the tt staggered form; according to theoretical calculations, in both i- and s-PMMA chains, the tt conformation is energetically the most favored.[18–20]

Important information concerning the structure of polymers in the amorphous and semicrystalline states can be obtained by means of high-resolution ^{13}C NMR spectra with simultaneous application of the dipolar decoupling, cross-polarization (CP), and magic-angle spinning (MAS) techniques.[21–23] Although atactic PMMA has been one of the first polymers used for demonstrating the ^{13}C CP/MAS NMR method,[24] the stereoregular forms of PMMA have been studied by this method and by ^{13}C T_1 relaxation times only by Edzes and Veeman.[25] In the work of these authors, the state of the samples is not clearly specified, but it may be assumed that they studied amorphous i- and s-PMMA. Simultaneously they also studied stereocomplex PMMA; in this case no remarkable differences were observed as compared to i- and s-PMMA alone, both in the appearance of ^{13}C CP/MAS NMR spectra and in the values of ^{13}C T_1 relaxation times.[25] The aim of this work was to determine whether differences exist between ^{13}C CP/MAS NMR spectra of stereoregular PMMA in amorphous and crystalline state and in a positive case to interpret the obtained results (including the measured values of $T_{1\rho}{}^{H}$ spin–lattice relaxation time in rotating frame for protons) in terms of the structural forms of amorphous and crystalline stereoregular PMMA.

Experimental Section

Methods. ^{13}C NMR spectra of CDCl$_3$ solutions of i- and s-PMMA (10% w/v) were measured with the spectrometer Varian XL-200 at 50.3 MHz and 25 °C, accumulating 3500 scans at a repetition interval of 8 and 4 s for i- and s-PMMA, respectively. Hexamethyldisiloxane (HMDS) with a signal at 2 ppm from TMS was used as internal standard. ^{13}C CP/MAS NMR spectra of solid PMMA samples were measured with the spectrometer Bruker MSL 200 at 50.3 MHz and ambient temperature. All solid samples were measured in Al$_2$O$_3$ rotors at identical conditions, suitable for producing difference spectra by computer treatment: number of scans, 12 000; spinning frequency, 4 kHz; decoupling field strength in frequency units (γH$_2$/
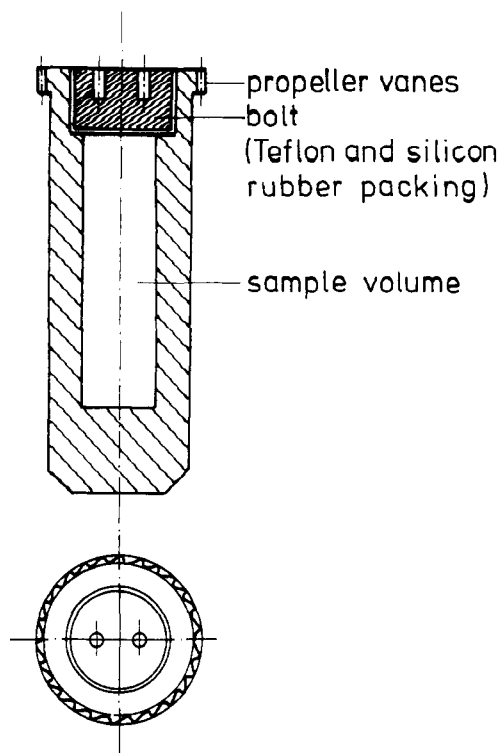
Figure 1. Schematic representation of the Delrin rotor used for the measurement of MAS NMR spectra of liquid and gel samples.

2π), 50 kHz; contact time, 2 ms; repetition time, 4 s; spectral width, 20 kHz; number of points, 8K. In some cases also the so-called nonquaternary suppression (NQS) spectra[26] were measured, suppressing the bands of ^{13}C nuclei with directly bonded protons, with the exception of such carbons in rapidly rotating groups (CH₃); in NQS spectral measurements, the measuring parameters were the same as in conventional CP/MAS spectra. Chemical shifts in ^{13}C CP/MAS NMR spectra were referred to the carbonyl band of glycine, with a signal at 176.0 ppm; the sample of glycine was repeatedly measured over a long period of time in 1- or 2-day intervals, and from these measurements the maximum instability limit of ±0.1 ppm was estimated. Considering that the digital resolution of our ^{13}C CP/MAS NMR spectra is also 0.1 ppm, then the estimated error in chemical shift determination does not exceed ±0.2 ppm. The intensities of partly overlapping bands were obtained by separation by means of the program GLINFIT. The values of the relaxation time $T_{1\rho}{}^{H}$ were determined (together with the values of the cross-polarization relaxation time, T_{CH}) from the dependence of the band intensity for the given carbon on contact time τ

$$I = (I_o/T_{CH})(\exp(-\tau/T_{1\rho}{}^{H}) - \exp(-\tau/T_{CH}))(1/T_{CH} - 1/T_{1\rho}{}^{H})^{-1}$$

(1)

which is valid[27] for $T_{1\rho}{}^{C} > T_{1\rho}{}^{H} \gg T_{CH}$; the values of $T_{1\rho}{}^{H}$ and T_{CH} were determined by a least-squares procedure using the program SIMFIT. ^{13}C MAS NMR spectra of solutions and gels of stereoregular PMMA were measured in Delrin (i.e., polyoxymethylene) rotors of our own construction, permitting the measurement of liquid or gel samples (Figure 1). These spectra were measured without CP; other parameters were similar as for the measurement of ^{13}C CP/MAS NMR spectra of solid samples: spinning frequency, 4.2 kHz; decoupling field, 45 kHz; number of scans, 12 000; repetition time, 5 or 10 s (to detect signals with possibly longer T_1).

Wide-angle X-ray scattering (WAXS) patterns were measured using the diffractometer HZG/4A (Präzisionsmechanik, Freiberg, GDR) and the flat-film camera with Cu Kα radiation and Ni filter. With the diffractometer, the diffracted radiation was recorded by means of a proportional counter.

Samples. Polymers: The polymer i-PMMA was prepared by anionic polymerization initiated with phenylmagnesium bromide in toluene at 17 °C. The polymer s-PMMA was prepared

Table I
Characterization of Crystalline Stereoregular PMMA Samples by WAXS

sample	degree of crystallinity, %	size of crystallites, nm
i-PMMA	40	9.0
s-PMMA	36	5.4
stereocomplex PMMA (i/s = 1/1.5)	40	5.2

by ion-coordination polymerization initiated with triethylaluminum and TiCl₄ in toluene at -78 °C. By ^1H NMR analysis (JEOL PS-100, 100 MHz, equimolar mixture of tetrachloroethylene with o-dichlorobenzene, 130°), i-PMMA contains more than 98% isotactic triads; s-PMMA contains 90% syndiotactic, 9% heterotactic, and 1% isotactic triads.

Amorphous and crystalline samples: By WAXS, the i-PMMA and s-PMMA samples prepared in the above-described way are amorphous. However, in order to clearly define the history of amorphous sample preparation, the amorphous i- and s-PMMA samples were prepared from acetonitrile solutions by evaporation of solvent;[5,14] by WAXS measurements it was confirmed that such samples are completely amorphous. The sample of crystalline s-PMMA was prepared by evaporation of solvent from a toluene solution (gel) at room temperature under vacuum.[1,5,14] The sample of crystalline i-PMMA was prepared by evaporation of solvent from an o-xylene gel at room temperature under vacuum.[9] The sample of crystalline stereocomplex PMMA was prepared by evaporation of solvent (at room temperature under vacuum) from a gel formed by mixing of acetonitrile solutions of i- and s-PMMA (the ratio of i-PMMA/s-PMMA was 1/1.5).[1,5,14] All crystalline samples contained a small amount of residual solvent (see also ref 5), detectable even in ^{13}C CP/MAS NMR spectra. The crystallinity degree was determined by WAXS; it was calculated as the ratio of the integral intensities of the scattering of the crystalline phase (obtained after separation of the amorphous component of scattering) to the total scattering, in the range of diffraction angles 2θ from 5° to 38°. The obtained crystallinity values, together with crystallite size data as determined from the broadening of crystalline reflections corrected for instrumental broadening, are summarized in Table I.

Results

^{13}C NMR Spectra of Stereoregular PMMA in Amorphous and Crystalline States. Although this work was primarily concerned with the measurement of ^{13}C NMR spectra of stereoregular PMMA in the solid state, ^{13}C NMR spectra of CDCl₃ solutions of the studied i- and s-PMMA samples are shown for comparison in Figure 2. The chemical shift values (shown in the spectrum in parentheses) are in good agreement with previously published data.[28]

^{13}C CP/MAS NMR spectra of amorphous (spectrum a) and crystalline (spectrum b) s-PMMA measured under identical conditions are shown in Figure 3. ^{13}C CP/MAS NMR spectra of amorphous (a) and crystalline (b) i-PMMA are shown in Figure 4. The spectra designated as c in Figures 3 and 4 were obtained from normalized spectra of crystalline samples (b) by subtraction of the spectra of the corresponding amorphous samples (a) multiplied by the factor f (fraction of the amorphous phase) adjusted so as to completely remove the bands of the amorphous component, without the appearance of any counterpeaks in the resulting spectrum. The found values $f = 0.6$ are in agreement with the crystallinity values obtained for crystalline s- and i-PMMA by WAXS (see Table I). The spectra c in Figures 3 and 4 thus represent ^{13}C CP/MAS NMR spectra of the crystalline phase of s- and i-PMMA, respectively.

Besides the bands of various PMMA carbons, the chemical shifts of which are shown in Table II, ^{13}C CP/MAS
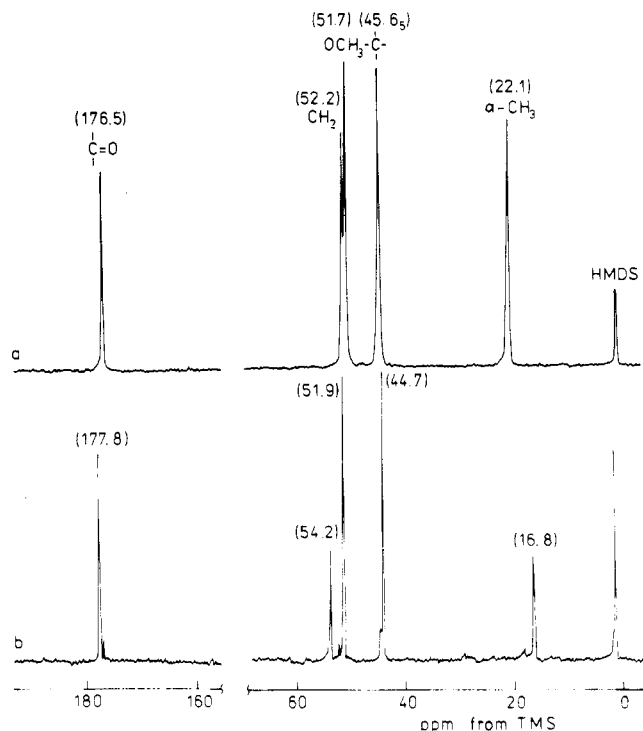
Figure 2. ^{13}C NMR spectra of CDCl$_3$ solutions of i-PMMA (a) and s-PMMA (b) measured at 50.3 MHz at room temperature. The numbers in parentheses are chemical shifts referred to TMS.
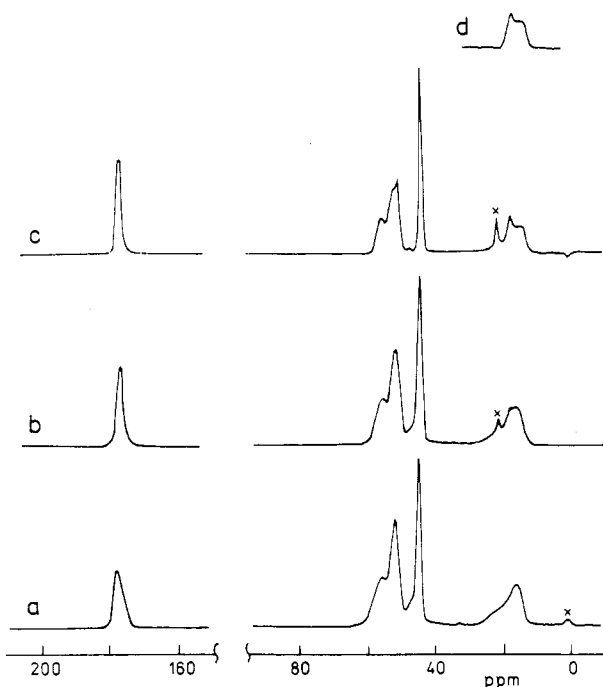

Figure 3. ^{13}C CP/MAS NMR spectra of amorphous s-PMMA (a) and of semicrystalline s-PMMA (b) measured at 50.3 MHz and room temperature. Spectrum c was obtained from spectrum b by subtraction of spectrum a multiplied by the factor f = 0.6, and it corresponds to purely crystalline state. A part of spectrum d was obtained from spectrum c by subtracting the band of residual toluene at 21.4 ppm. Bands of residual solvent are designated by ×.

NMR spectra of solid PMMA also exhibit bands of residual solvents (see the Experimental Section). Thus the band at ~0.9 ppm in the spectra of amorphous s-PMMA (Figure 3a) and amorphous i-PMMA (Figure 4a) corresponds to the methyl carbons of residual acetonitrile;[29] in spectra c of Figures 3 and 4, this band appears as a
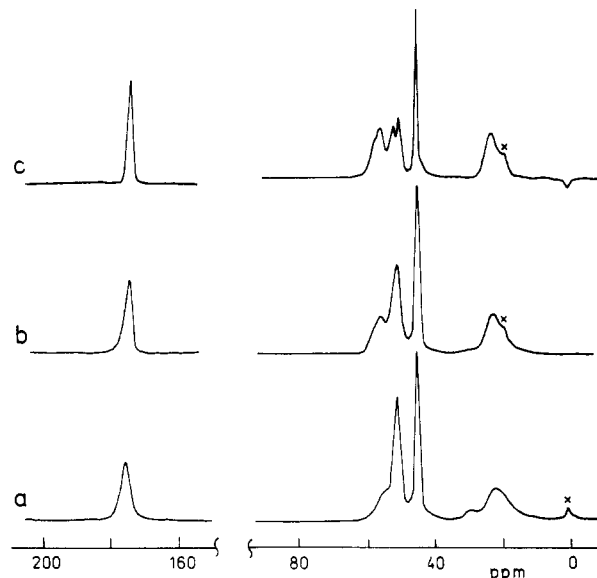

Figure 4. ^{13}C CP/MAS NMR spectra of amorphous i-PMMA (a) and of semicrystalline i-PMMA (b) measured at 50.3 MHz and room temperature. Spectrum c was obtained from spectrum b by subtracting spectrum a multiplied by the factor f = 0.6 and corresponds to purely crystalline state. Bands of residual solvent are designated by ×.

Table II
^{13}C Chemical Shifts of Stereoregular PMMA in Amorphous and Crystalline State (ppm from TMS)

sample	C=O	CH$_2$	OCH$_3$	$-\overset{\mid}{\underset{\mid}{C}}-$	α-CH$_3$
i-PMMA amorphous	175.9	55.2	51.7	45.4	22.8 30.0
i-PMMA cryst phase[a]	174.7	56.8 58.3	50.95 52.4	45.8	23.7
s-PMMA amorphous	177.7	55.7	51.6	44.45	15.7 21.9
s-PMMA cryst phase[a]	177.4	55.3	50.7 51.9	44.1	15.25 17.7
stereocomplex[a,b]	178.65 (s)	59.2 (i)	51.8	45.4	24.4 (i)
PMMA cryst phase	175.55 (i)	54.15 (s)			14.85 (s)

[a] Values obtained from ^{13}C CP/MAS NMR spectra of crystalline sample by substracting the amorphous component. [b] (s) and (i) denote band assignment to the respective PMMA chains.

counterpeak. The sharp band at 21.4 ppm (Figure 3b,c), the broader band at 129 ppm, and the weak band at 137 ppm in the spectra of crystalline s-PMMA correspond to residual toluene.[29] Similarly, the band at 19.7 ppm (appearing as a shoulder on the α-CH$_3$ carbon band) (Figure 4b,c) and the weak bands in the range 125–137 ppm (overlapping the spinning sidebands) in the spectra of crystalline i-PMMA correspond to residual o-xylene.[29,30]

When ^{13}C NMR spectra of amorphous s-PMMA (Figure 3a) and i-PMMA (Figure 4a) samples are compared with the solution spectra of these two samples, we observe the greatest difference in the range of the α-CH$_3$ resonance of i-PMMA, where amorphous i-PMMA exhibits two bands at 22.8 and 30 ppm, whereas the corresponding CDCl$_3$ solution exhibits a single band at 22.1 ppm. Analysis of expanded spectra revealed that the band of amorphous i-PMMA at 22.8 ppm corresponds to 89% of the integrated intensity of α-CH$_3$ carbons, and the band at 30.0 ppm, to 11% of this intensity. A similar, though less pronounced effect was observed also with the α-CH$_3$ resonance of amorphous s-PMMA (Figure 3a). In this case the α-CH$_3$ carbon resonance exhibits a very asymmetrical shape, with a peak at 15.7 ppm and a shoulder

at 21.9 ppm indicating the presence of a considerably weaker second band.

Marked differences are also observed when ^{13}C NMR spectra of the crystalline phase in s-PMMA (Figure 3c) are compared with the spectrum of amorphous s-PMMA (Figure 3a). While the band shape and chemical shifts (Table II) of carbonyl, methylene, and quaternary carbon signals do not practically differ in purely crystalline and amorphous s-PMMA, in the range of α-CH_3 resonance the spectra of the crystalline phase clearly exhibit two bands of approximately equal intensity at 15.25 and 17.7 ppm; also the OCH_3 carbon resonance is split (bands at 50.7 and 51.9 ppm) in the crystalline phase. At the same time, the chemical shifts of 15.25 and 51.9 ppm roughly correspond to the chemical shifts of α-CH_3 and OCH_3 carbons in amorphous s-PMMA (Table II).

In ^{13}C NMR spectra of the crystalline (Figure 4c) and amorphous (Figure 4a) phases of i-PMMA, only quaternary carbons exhibit the same chemical shifts (Table II) and equal line shapes in both cases. The OCH_3 carbon band in the crystalline phase of i-PMMA is split into two bands (50.95 and 52.4 ppm), roughly symmetrically placed about the OCH_3 resonance in amorphous i-PMMA (51.7 ppm). A shoulder (at 58.3 ppm) indicating the presence of two bands is observed also at the CH_2 resonance in the crystalline phase of i-PMMA, with a peak at 56.8 ppm. In this case both these bands occur at a slightly lower field than in amorphous i-PMMA; the situation is similar for α-CH_3 carbons. On the other band, the carbonyl band in crystalline i-PMMA is shifted by about 1.2 ppm to higher field, as compared to amorphous i-PMMA.

The ^{13}C CP/MAS NMR spectrum of a solid stereocomplex PMMA sample prepared by evaporation of solvent from a mixture of acetonitrile i- and s-PMMA solutions (i/s = 1/1.5) is shown in Figure 5a. Similarly as in the spectra of amorphous i- and s-PMMA samples, also in this case the CH_3 carbon signal of residual acetonitrile was detected at 0.9 ppm. The ratio i/s = 1/1.5 is cited as the stoichiometric ratio of i- and s-units in the ordered stereocomplex structure.[1,31,32] As the solutions of i- and s-PMMA had been mixed in this ratio, the composition not only of the crystalline but also of the amorphous phase of the stereocomplex should correspond to this stoichiometry. The ^{13}C NMR spectrum of the crystalline phase of the stereocomplex, derived from the measured spectrum (Figure 5a) by subtracting the spectrum of the amorphous phase multiplied by the factor 0.6, is shown in Figure 5c; for this purpose, the spectrum of the amorphous phase was constructed from the spectra of amorphous i- and s-PMMA with the ratio i/s = 1/1.5. Similarly as in the previously described cases of the crystalline phases of s- and i-PMMA, also here the optimized fraction of f of the amorphous phase is in very good agreement with the crystallinity degree as determined by WAXS (Table I). The sum spectra of amorphous i- and s-PMMA composed in the ratio i/s = 1/1.5 (Figure 5d) and of the crystalline phases of i- and s-PMMA (see Figures 3c and 4c) added in the same i/s ratio (Figure 5e) are also shown for comparison. In the sum spectrum of the crystalline phases, the shape of the α-CH_3 range is disfigured to some extent by the presence of residual toluene and o-xylene bands in the spectra of the crystalline phases of s- and i-PMMA, respectively. As in some cases where the stoichiometry of the stereocomplex is given as i/s = 1/2,[1,33] we have analyzed the measured ^{13}C CP/MAS NMR spectrum of the PMMA stereocomplex sample also for this composition of the crystalline phase;
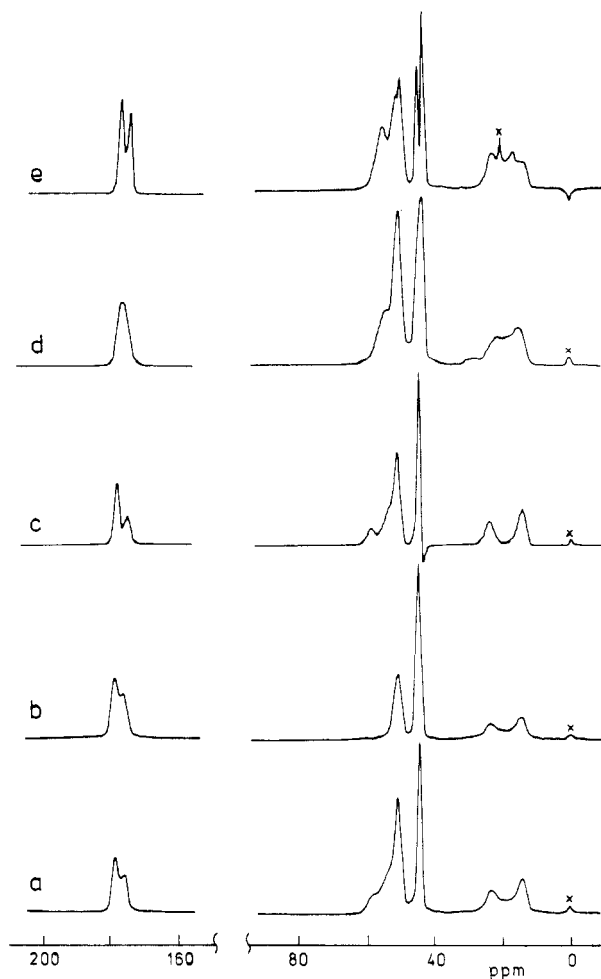

Figure 5. ^{13}C CP/MAS NMR spectra of stereocomplex PMMA measured at 50.3 MHz and room temperature (a,b). Spectrum b was measured by the NQS technique. Spectrum c was obtained from spectrum a by subtracting the normalized sum spectrum of amorphous i- and s-PMMA in the ratio i/s = 1/1.5 (d) multiplied by the factor f = 0.6 and corresponds to purely crystalline state. Spectrum e represents the sum spectrum of the crystalline phases of i- and s-PMMA (see Figures 3c and 4c) composed in the ratio i/s = 1/1.5. Bands of residual solvent are designated by ×.

it could be shown that in this case the composition of the amorphous phase of our sample would be i/s = 1/1.25. We have also found that, for the stoichiometry i/s = 1/2, the spectrum of the crystalline phase of the stereocomplex is practically identical with the spectrum in Figure 5c; corresponding to the stoichiometry i/s = 1/1.5, only the relative intensities of the bands of i- and s-units (see further text) are slightly different.

The spectrum of the stereocomplex (Figure 5a,c) exhibits band pairs in the ranges of α-CH_3 and C=O carbons; these evidently correspond to s-units (stronger band) and i-units (weaker band). Their chemical shifts either roughly agree (α-CH_3) or are slightly shifted downfield (C=O) as compared to the corresponding bands of crystalline i- and s-PMMA; however, the α-CH_3 band of crystalline s-PMMA at 17.7 ppm is not detected in the spectrum of the crystalline stereocomplex. The most conspicuous difference is observed already in the experimental spectrum of the stereocomplex (a) and is even more pronounced in the spectrum of purely crystalline stereocomplex (c) in the range of the CH_2 resonance, where, besides the band at 54.1 ppm, also a band at 59.2 ppm is detected. As CH_2 carbon resonance occurs in the near vicinity of OCH_3 resonance, the NQS technique was applied for the unambiguous assignment of the band at 59.2 ppm (by

the NQS technique, bands of carbons with directly bonded protons (CH_2) are suppressed, with the exception of rapidly rotating groups (CH_3)). The NQS spectrum of a stereocomplex sample is shown in Figure 5b. It may be seen that, in the 50–60 ppm range, only the band of OCH_3 carbons at 51.6 ppm has been preserved; bands at 54.1 and 59.2 ppm disappeared, clearly indicating that both these bands should be assigned to CH_2 carbons. The possibility of the occurrence of two CH_2 carbon bands in the ^{13}C NMR spectrum of crystalline stereocomplex (Figure 5c) is supported by the observation that the shape of the bands in this range remains the same in measurements with a contact time of 2 ms (Figure 5a) and of 50 μs; the rigid crystalline phase should be preferred by the latter.[22,23] After separation of the OCH_3 band, the ratio of integrated intensities of the bands at 59.2 and 54.1 ppm is ~1/1.7, i.e., very near to the stoichiometric i/s ratio. Therefore, it may be assumed that the band at 54.1 ppm in the crystalline stereocomplex corresponds to CH_2 groups in s-units; its chemical shift does not differ much from the chemical shift of CH_2 carbons in crystalline s-PMMA (Table II). The band at 59.2 ppm most probably corresponds to CH_2 groups in i-units; its position is near to the position of the shoulder at 58.3 ppm in crystalline i-PMMA (Table II). The position of the OCH_3 band in crystalline stereocomplex is equal to that in other PMMA samples. Also the quaternary carbon exhibits a single band in the ^{13}C NMR spectrum of the stereocomplex, indicating that, contrary to the crystalline phases of i- and s-PMMA (see Figure 5e and Table II), in crystalline stereocomplex the quaternary carbons of i- and s-units resonate at the same field.

Besides ^{13}C NMR spectra of crystalline and amorphous i- and s-PMMA, also the ^{13}C NMR spectra of an s-PMMA gel in toluene-d_8 were measured in a special Delrin rotor. In this solvent, s-PMMA forms ordered aggregated structures; ^1H NMR measurements have indicated that 75–85% of s-PMMA units are present in the aggregated state.[1,15,34] In ^1H NMR spectra, the bands of these units exhibit a width of 500 ± 100 Hz, so that, in conventionally measured ^1H or ^{13}C NMR spectra, these aggregated units escape detection.[34] We have compared ^{13}C NMR spectra of s-PMMA in toluene-d_8 with ^{13}C NMR spectra of a solution of s-PMMA in $CDCl_3$ measured under identical conditions; it is well-known that, in chloroform, aggregated s-PMMA structures do not exist.[1] In both cases ^{13}C CP/MAS NMR spectra exhibited only very weak bands, indicating that, in the toluene gel of s-PMMA, similarly as in the $CDCl_3$ solution, cross-polarization has very little effect. Therefore, we have measured ^{13}C MAS NMR spectra of these systems with strong proton decoupling ($\gamma H_2/2\pi \cong 45$ kHz) without cross-polarization (Figure 6). From Figure 6 it is evident that the band intensities of all carbons of s-PMMA in toluene-d_8 are considerably lower than those for s-PMMA in $CDCl_3$. When the integrated intensity of a given band for s-PMMA in $CDCl_3$ is set equal to 100%, then for s-PMMA in toluene-d_8 the integrated intensity amounts to only 30 ± 5%. This result is independent of the repetition time and thus is not caused by possible differences in the T_1 relaxation times of the aggregated and nonaggregated phases of s-PMMA. This indicates that, in ^{13}C MAS NMR spectra with strong proton decoupling, the nonaggregated phase is predominantly detected, similarly as in conventional ^1H and ^{13}C NMR spectra. Even in ^{13}C MAS NMR spectra measured in this way, carbon bands of the aggregated fraction escape detection.

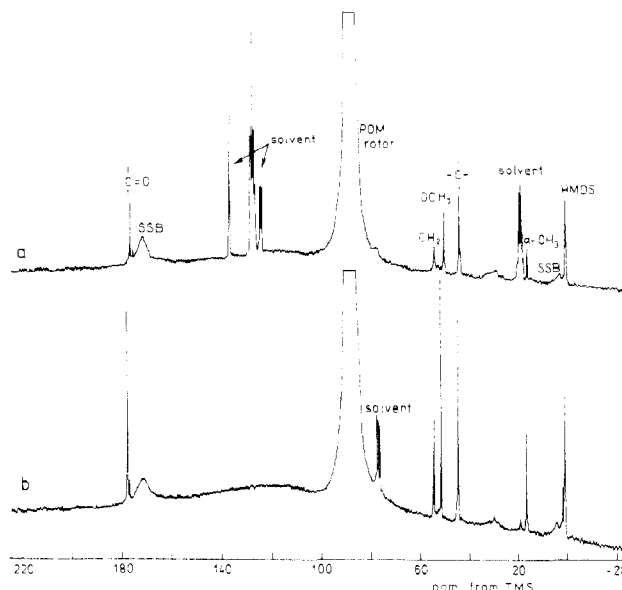**Values of $T_{1\rho}{}^H$ in Stereoregular PMMA.** The depen-

Figure 6. ^{13}C MAS NMR spectra of s-PMMA in toluene-d_8 (a) and in $CDCl_3$ (b) measured at 50.3 MHz, room temperature, and identical instrumental setting. In both cases the concentration of s-PMMA was 10% w/v. SSB designates spinning side bands.

dences of the intensity of a given band on the contact time τ, from which the relaxation times $T_{1\rho}{}^H$ and the cross-polarization relaxation times T_{CH} have been determined, are demonstrated on the examples of amorphous and crystalline i-PMMA in Figure 7. We have found that in all cases (i.e., also for amorphous and crystalline s-PMMA and for stereocomplex PMMA) these dependences can be analyzed with a single $T_{1\rho}{}^H$ and a single T_{CH} value (i.e., using relation 1) only in the case of nonprotonated, i.e., quaternary and carbonyl carbons. The dependences for the protonated carbons could in first approximation be described by considering two components of the relaxation time T_{CH}, $T_{CH}{}^A$ and $T_{CH}{}^B$, so that relation 1 had to be replaced by

$$I = (I^A + I^B) \exp(-\tau/T_{1\rho}{}^H) - (I^A \exp(-\tau/T_{CH}{}^A) + I^B \exp(-\tau/T_{CH}{}^B)) \quad (2)$$

where

$$I^A = I_0{}^A(1 - T_{CH}{}^A/T_{1\rho}{}^H)^{-1}$$

$$I^B = I_0{}^B(1 - T_{CH}{}^B/T_{1\rho}{}^H)^{-1}$$

This is evidently in relation to the circumstance that, for the protonated carbons, the dynamics of cross-polarization proceeds in two steps: first as coherent energy transfer between the carbon and its bound protons and second as cross-relaxation energy transfer from this group to more distant protons.[35]

For carbonyl and quaternary carbons, the found T_{CH} values were roughly equal (within experimental error) for the whole studied sample series and were equal to 700–850 μs for carbonyl carbons and to 250–320 μs for quaternary carbons. For all protonated carbons, a short and a long T_{CH} component was found, and the corresponding intensities ($I_0{}^A$ and $I_0{}^B$) were mostly comparable. The intensity dependence on contact time for CH_2 carbons could only be analyzed with crystalline i- and s-PMMA, where the CH_2 and OCH_3 bands are well resolved (see Figures 3b and 4b); in other cases the intensity determination for the CH_2 band is subject to considerable error due to insufficient separation of CH_2 and OCH_3 bands.
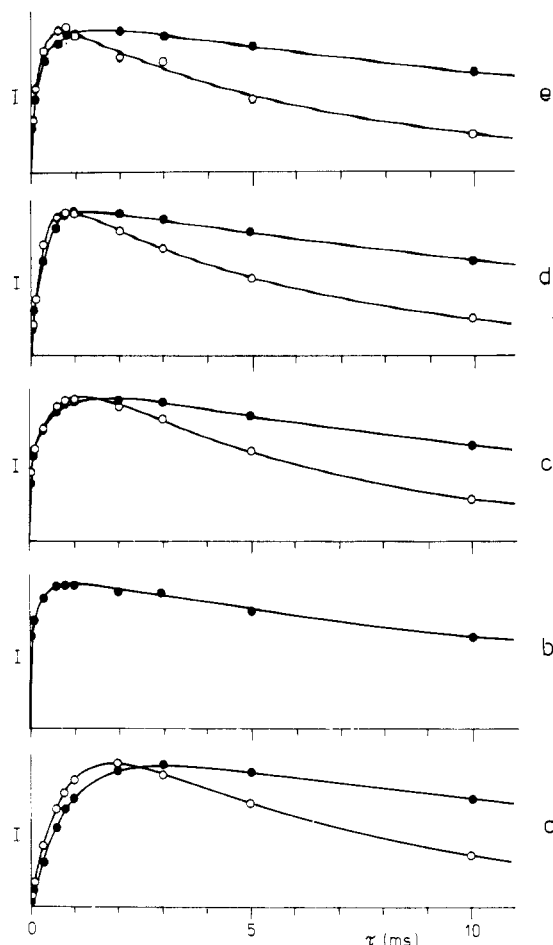
Figure 7. Dependence of band intensity on contact time, τ, for C=O (a), CH_2 (b), OCH_3 (c),)C((d) and α-CH_3 (e) carbons in amorphous (open symbols) and crystalline (full symbols) i-PMMA. The symbols correspond to experimental points, the full lines represent the best fit obtained by the method of least squares assuming one $T_{1\rho}{}^H$ and one T_{CH} (a,d) or one $T_{1\rho}{}^H$ and two T_{CH} components (b,c,e).

Both with crystalline i-PMMA and with crystalline s-PMMA for CH_2 carbons the obtained values were T_{CH} $\approx$ 20 μs for the short component and T_{CH} $\approx$ 260 μs for the long component. The value T_{CH} $\approx$ 20 μs has been previously observed for CH_2 carbons in amorphous atactic PMMA.[24] With the stereocomplex sample, T_{CH} values could be determined for α-CH_3 carbons in i- and s-PMMA chains (see Figure 5a). We have found that the long T_{CH} component in this case is practically equal to that in the corresponding crystalline i- or s-PMMA and amounts of 500 μs for i-chains and to 840 μs for s-chains. The short T_{CH} component of α-CH_3 carbons is equal (105 μs) for i- and s-PMMA chains in the stereocomplex, but it is somewhat longer than the short T_{CH} component found for α-CH_3 carbons in crystalline i-PMMA (80 μs) or crystalline s-PMMA (60 μs).

The values of the $T_{1\rho}{}^H$ relaxation time determined for the studied sample series are shown in Table III. Besides the previously described sample of stereocomplex PMMA prepared from a mixture of acetonitrile solutions of i- and s-PMMA (ratio i/s = 1/1.5) exhibiting 40% crystallinity by WAXS, Table III also includes values for a stereocomplex sample prepared from a mixture of dimethylformamide solutions (ratio i/s = 1/2); for unknown reasons, this sample exhibited a crystallinity of only 16% by WAXS. It is evident from Table III that, with all studied samples, the $T_{1\rho}{}^H$ values determined from an analysis of various carbon bands are equal within experimental error, due to the spin-diffusion mechanism, as was to

be expected.[21,22] Only the $T_{1\rho}{}^H$ value found for the α-CH_3 carbons of amorphous s-PMMA is significantly shorter. It is interesting that also Jo et al.[36] cite a similar significantly shorter value of $T_{1\rho}{}^H$ (9.8 ms) for the α-CH_3 carbons of conventional PMMA. For partially crystalline samples of i-PMMA, s-PMMA, and stereocomplex PMMA, only a single $T_{1\rho}{}^H$ value was found by an analysis of intensity dependences for all carbon types, similarly as with amorphous samples. For these samples it was also possible to describe the dependence of intensity on contact time, by artificially introducing two $T_{1\rho}{}^H$ components. The values of the longer component were only slightly higher than the single $T_{1\rho}{}^H$ values shown for the given semicrystalline sample in Table III. The intensity of the shorter component was always very small and did not exceed several percent, at variance with the content of the amorphous fraction as determined for semicrystalline PMMA by WAXS (cf. Table I).
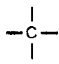
From Table III it may be seen that the smallest $T_{1\rho}{}^H$ value was found for amorphous i-PMMA; in contrast, crystalline i-PMMA exhibits the highest $T_{1\rho}{}^H$ value. $T_{1\rho}{}^H$ values for amorphous and crystalline s-PMMA are comparable. For stereocomplex PMMA samples it was possible to selectively determine $T_{1\rho}{}^H$ values for i- and s-PMMA chains from an analysis of the dependence of the intensities of carbonyl or α-CH_3 carbon bands on contact time. These values were found to be equal and to differ from those of the individual stereoregular PMMA.

Discussion

1. ^{13}C NMR Spectra and Conformational Structure of the Amorphous or Crystalline States in Stereoregular PMMA. Amorphous i- and s-PMMA. As explained above, in the range of α-CH_3 resonance, amorphous i-PMMA exhibits, besides the band at 22.8 ppm roughly corresponding to the position of the α-CH_3 band of i-PMMA in solution, a further band at 30 ppm; the integrated intensity of this band corresponds to 11% of the total intensity of the α-CH_3 carbon resonance. The weak band of i-PMMA at $\sim$30 ppm has already been observed by Edzes and Veeman[25] who assigned it to trapped solvent molecules. However, in our case it is quite clear that the band at 30 ppm is not due to solvent, as no such band has been detected in the solution spectrum of i-PMMA (Figure 2a). At the same time, Figure 4 demonstrates that the intensity of this band is substantially lower in the experimental spectrum of partially crystalline i-PMMA (Figure 4b); this band disappears completely after subtraction of the spectrum of the amorphous phase (Figure 4c). Therefore, it may be stated that the α-CH_3 carbon band at 30 ppm is characteristic of amorphous i-PMMA.

Chemical shift differences observed in ^{13}C CP/MAS NMR spectra may be connected with conformational structure in consequence of the so-called γ-gauche effect.[22,23] Local conformation is defined by the positions of the so-called γ-carbons, i.e., carbons removed by three bonds from the observed carbon. In consequence of the γ-effect, a change in conformation from trans to gauche causes a change in chemical shift toward higher field. The extent of this effect may be highly variable; usually it amounts to 3.5–5 ppm for one γ-carbon. For more γ-carbons, the resulting effect is additive.[22] In the case of PMMA it may be assumed that the γ-gauche effect will be combined with the effect of C=O bonds, so that the resulting change in chemical shift due to conformational change may be even higher. As stated in the Introduction, both theoretical studies[18-20] and WAXS measurements[10,11,37] indicate that the tt conformational back-

Table III
Values of Proton Spin–Lattice Relaxation Time in Rotating Frame, $T_{1\rho}{}^H$, Determined from Proton–Carbon Cross-Polarization at $\gamma H_1/2\pi = 50$ kHz and Room Temperature

| sample | $T_{1\rho}{}^{H,a}$ ms | | | | | |
	C=O	CH₂	OCH₃	—C—	α-CH₃	mean value
i-PMMA amorphous	7.1	*b*	6.7	6.3	6.7	6.7
i-PMMA semicrystalline	23.0	20.1	19.5	21.0	20.9	20.9
s-PMMA amorphous	18.9	*b*	17.7	18.7	10.4	18.4[g]
s-PMMA semicrystalline	17.0	15.4	15.5	16.8	13.0[c] 12.7[d]	15.5
stereocomplex PMMA (crystallinity degree 16%)	13.8 (s)[e] 13.3 (i)[f]	*b*	13.3	14.7	13.0 (s)[e] 12.5 (i)[f]	13.6
stereocomplex PMMA (crystallinity degree 40%)	16.1 (s)[e] 16.2 (i)[f]	*b*	16.3	17.3	14.8 (s)[e] 14.8 (i)[f]	16.1

[a] Estimated error ±10%. [b] Not measured due to insufficient separation of CH₂ carbon band. [c] Band of α-CH₃ carbons at 15.25 ppm. [d] Band of α-CH₃ carbons at 17.7 ppm. [e] Band of s-PMMA chains. [f] Band of i-PMMA chains. [g] Value from α-CH₃ carbon analysis not included.
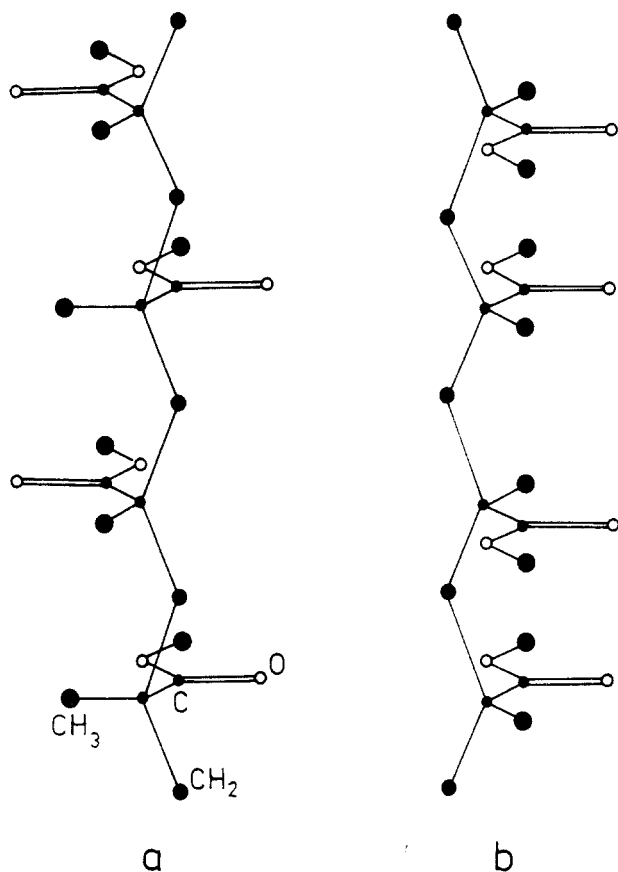

Figure 8. Schematic representation of the tt conformational structure of i-PMMA with ester groups alternatively in syn (cis) and anti (trans) orientation (a); schematic representation of tt conformational structure of s-PMMA with ester groups in syn (cis) orientation (b).

bone structure schematically shown in Figure 8a predominates not only in crystalline but also in amorphous i-PMMA; however, amorphous i-PMMA also contains some fraction of tg and gt conformational diads. For the t backbone conformation, the mutual orientation of α-CH₃ carbons and γ-carbons (quaternary carbon) is gauche. For the g backbone conformation (generated by rotation about the C_α–CH₂ bond), the mutual orientation of the α-CH₃ and quaternary carbons is changed to trans (in the other gauche backbone conformation ḡ, the orientation of the α-CH₃ and quaternary carbons is gauche, but this conformation usually is excluded on energy considerations[38]). Therefore, we assume that the observed two α-CH₃ bands

of amorphous i-PMMA correspond to t (22.8 ppm) and g (30 ppm) backbone conformational structures. The relative intensity of the band at 30 ppm (11%) agrees well with the probability of the g conformation, $w_g = 0.13$ as determined from conformational analysis and dipole moments of i-PMMA.[38] A similar splitting might also be expected for the CH₂ carbons; however, in this case the CH₂ carbon band corresponding to g conformational structures would lie at higher field than the band of the dominating t structures. Such a CH₂ band has not been detected, but due to its presumed overlap with the OCH₃ carbon band (Figure 4a) and small intensity, its existence cannot be excluded. We have also considered the possibility that the chemical shift of the α-CH₃ band could hypothetically be affected by the orientation of the ester group, when the C–CH₃ and C=O bonds can assume the cis (syn) or trans (anti) orientation.[1] This, however, is clearly contradicted by the intensities of both observed α-CH₃ bands in ¹³C CP/MAS NMR spectra, which evidently disagree with the conclusions of refs 20 and 38, which indicate a regular alternation of cis and trans ester group orientation in i-PMMA.

Two α-CH₃ carbon bands separated by 6.2 ppm (at 15.7 and 21.9 ppm) were also observed with amorphous s-PMMA (Figure 3a, Table II). In the spectrum of the crystalline phase of s-PMMA this range is obscured by the band of residual toluene (Figure 3c); when this is subtracted, it becomes clear that the band at 21.9 ppm is not present (Figure 3d). Due to the nonnegligible content of heterotactic triads in this sample (9%), two α-CH₃ bands are observed also in the solution spectrum (Figure 2b); however, the chemical shift difference between α-CH₃ carbon signals of syndiotactic and heterotactic triads in CDCl₃ solution amounts to only 2 ppm[28] (see also Figure 2b). Similarly, Tanaka et al.[39] report on the basis of ¹³C CP/MAS NMR measurements of atactic PMMA that the chemical shift difference between heterotactic and syndiotactic triads is only 2.4 ppm. As the content of isotactic triads in s-PMMA is negligible (1%), the α-CH₃ band at 21.9 ppm evidently cannot be assigned to isotactic triads. Similarly, as in the case of i-PMMA, also for s-PMMA both theoretical and experimental results indicate that the tt backbone conformation dominates also in amorphous s-PMMA; tg conformational diads are present in a smaller amount.[1,18,19,38,40,41] The effect of backbone conformational structure in s-PMMA on α-CH₃ carbon resonance is expected to be similar to that in i-PMMA; i.e., with the backbone t conformation, the qua-

ternary γ-carbons will be in gauche orientation with respect to the α-CH₃ carbon and will cause its signal to be shifted toward higher field, as compared to the α-CH₃ carbons signal for the backbone gauche conformation where the mutual orientation of α-CH₃ and quaternary carbons is trans. Therefore, we assume that even with s-PMMA the shoulder on the α-CH₃ carbon band at 21.9 ppm is predominantly caused by the presence of backbone g conformational structures; however, heterotactic triads present in the studied sample contribute somewhat to its intensity. We also assume that, in atactic PMMA, such as studied e.g., by Tanaka et al.,[39] the shape of the α-CH₃ band is affected by presence of gauche conformational structure, even more so than in s-PMMA.

Crystalline Forms of Stereoregular PMMA. High-resolution ¹³C NMR spectra of the crystalline and amorphous phases of stereoregular PMMA exhibit significant differences. In the crystalline phase we mainly observe the splitting of some carbon bands into two components of comparable intensity (α-CH₃ and OCH₃ bands in crystalline s-PMMA and OCH₃ and possibly also CH₂ bands in crystalline i-PMMA) (Figures 3 and 4, Table II). The splitting of the two components amounts to 1.2–2.5 ppm. With i-PMMA we also observe differences in the chemical shifts of a given carbon in the crystalline and amorphous phase (carbonyl, CH₂, and α-CH₃ carbons), amounting to 1–3 ppm. In ¹³C NMR spectra of the crystalline stereocomplex we observe band pairs corresponding to i- and s-chains for carbonyl, α-CH₃, and very probably also CH₂ carbons (Figure 5c). From a comparison of spectra c–e in Figure 5 and from Table II it is evident that, even with the stereocomplex, the chemical shifts of i- and s-chains differ from the values in the corresponding amorphous or crystalline phases. For s-chains in the stereocomplex (C=O, CH₂, quaternary, and α-CH₃ carbons), chemical shifts differ from those of the amorphous phase by 1–1.5 ppm; for i-chains (CH₂ and α-CH₃ carbons) by 1.5–4 ppm. Even with respect to the crystalline phase, the chemical shifts of C=O and CH₂ and for s-chains also of quaternary carbons differ by ~1 ppm.

In the crystalline state a defined conformational structure dominates (in our case it is very near to the tt form[1]), and therefore it is clear that the observed splitting of some bands in the crystalline phase cannot be connected with backbone conformational structure. As band splittings and chemical shift differences are observed for various carbons, while the orientation of the ester group (cis or trans) would mostly affect the chemical shift of α-CH₃ carbons, the connection of the observed effects with the orientation of ester groups in i- or s-PMMA is also very improbable. On the other hand, the size of the chemical shift differences (mostly 1–2 ppm) indicates a possible effect of intermolecular polymer chain packing in the crystal.[23] As mentioned in the Introduction, a 10/1 double helix has been proposed for crystalline i-PMMA[10,11] based on X-ray diffraction. The structure of a double helix formed from i- and s-PMMA chains has been proposed also for stereocomplex PMMA[1,12–14] based on X-ray, NMR, and IR measurements. We think that the mentioned splitting of some bands, as well as chemical shift differences with respect to the amorphous state are due to the existence of the double helices. The quite identical chemical shift values of quaternary carbons of the i- and s-chains in the stereocomplex (Figure 5, Table II) imply an at least very similar backbone conformational structure of these chains. Although even for crystalline s-PMMA indirect evidence indicates the formation of double helices with a large number of units per turn,[1,14–17]
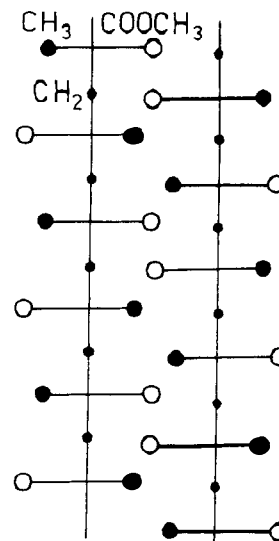

Figure 9. Schematic representation of two syndiotactic sequences with tt conformation in mutual interaction.

X-ray diffraction cannot clearly decide between a single or a double (possibly multiple) helix in this case.[6] In our opinion, the observed splitting of α-CH₃ and OCH₃ bands in ¹³C NMR spectra of crystalline s-PMMA supports the assumption that double-helical structures also occur in crystalline s-PMMA. When two s-chains in mutual interaction are approximated by the extended chain tt conformation (the conformational structure of a tt chain and of a chain forming a helix with a large number of units per turn is very near), then the schematic representation in Figure 9 indicates the existence of two types of α-CH₃ and OCH₃ carbons, internal and external, with somewhat differing chemical shifts and equal band intensities. The observed differences in ¹³C NMR spectra (Figures 3–5, Table II) indicate differences in the structure of the three basically similar (all form double helices) crystalline forms of stereoregular PMMA, i.e., of i-PMMA, s-PMMA, and stereocomplex PMMA. We believe that analysis of these spectra will in the future provide more detailed information on the structure of crystalline PMMA.

s-PMMA Gels. In addition to the solid PMMA samples, we have also measured ¹³C MAS NMR spectra of the toluene gel of s-PMMA in which 75–85% of s-PMMA units form aggregated structures. The finding that even in ¹³C MAS NMR spectra measured with strong proton decoupling most of the aggregated fraction cannot be detected confirms the results of our previous experiments based on the measurement of ¹H MAS NMR spectra and conventional ¹³C NMR spectra[34] and indicates that near-static dipolar interactions do not operate in s-PMMA aggregates. The motion of aggregated segments is spatially isotropic, with an effective correlation frequency of 10⁶–10⁷ Hz.[34] In our previous study, the same conclusion was reached also for gels of stereocomplex PMMA.[13]

2. Values of $T_{1\rho}^H$ and Dynamic Structure of Stereoregular PMMA. With all studied samples (amorphous and crystalline) always only a single $T_{1\rho}^H$ value was obtained within experimental error from the measurement of various carbons. Thus in partly crystalline i- and s-PMMA samples, different $T_{1\rho}^H$ values have not been found for the amorphous and crystalline phases, such as was the case, e.g., with poly(ethyleneterephthalate).[42] This indicates that, even in crystalline i-PMMA (where the largest crystallite size, 9 nm, is indicated by WAXS, see Table I), the size of crystalline domains is insufficient to affect the spin-diffusion pro-

cess averaging the relaxation behavior over the whole proton population, i.e., comprising both the amorphous and the crystalline phases.

When we compare the $T_{1\rho}{}^H$ values for amorphous i- and s-PMMA (Table III), we see that the $T_{1\rho}{}^H$ value is substantially smaller for i-PMMA. As at room temperature both polymers are below their T_g temperatures (T_g = 45 °C for i-PMMA and 115 °C for s-PMMA[43]), it may be expected that we operate in the low-temperature part of the relaxation curve where a higher $T_{1\rho}{}^H$ corresponds to lower mobility (longer correlation time). Thus the shorter $T_{1\rho}{}^H$ values found for i-PMMA, as compared to s-PMMA, are in agreement with the known higher mobility of the i-PMMA backbone.[1,43,44] While amorphous and partly crystalline i-PMMA samples exhibit widely differing $T_{1\rho}{}^H$ values (and consequently mobility) (Table III), for amorphous and partly crystalline s-PMMA, comparable $T_{1\rho}{}^H$ (and mobility) values are observed. A single $T_{1\rho}{}^H$ value, equal for the protons of i- and s-PMMA chains, was also obtained in the case of stereocomplex PMMA (Table III). At the same time, the stereocomplex of higher crystallinity (40%) exhibits a longer $T_{1\rho}{}^H$ than the stereocomplex of 16% crystallinity; in both these cases the found $T_{1\rho}{}^H$ values differ from those found for amorphous or partly crystalline samples of only i- or only s-PMMA. These results indicate that, in the stereocomplex, the i- and s-chains are intimately mixed and support the above-discussed structure of double helices composed of i- and s-PMMA chains.

Conclusions

Measurements of ^{13}C CP/MAS NMR spectra of amorphous and partially crystalline samples of i- and s-PMMA and of a sample of partially crystalline stereocomplex PMMA enabled us to obtain by a computer difference technique high-resolution ^{13}C NMR spectra of the crystalline phase of i- and s-PMMA and of the crystalline phase of stereocomplex PMMA. The observed two bands of α-CH$_3$ carbons in amorphous i-PMMA were assigned to trans and gauche backbone conformational forms; the relative intensities of these bands are in good agreement with the content of trans and gauche forms found in the literature. Likewise, the unusual shape of the α-CH$_3$ band of s-PMMA is interpreted by the presence of some amount of gauche conformational forms. We think that even the anomalous shape of the α-CH$_3$ band of atactic PMMA can be explained in this way. ^{13}C NMR spectra of crystalline forms of stereoregular PMMA differ in a characteristic manner from the spectra of the corresponding amorphous samples: By the splitting of some bands into two components of comparable intensity and by differences in the values of some chemical shifts. The ^{13}C NMR spectrum of the crystalline stereocomplex significantly differs from the sum spectrum of amorphous or crystalline i- and s-PMMA. The observed differences in the spectra of the amorphous and crystalline phase of stereoregular PMMA are caused by intermolecular interactions of chains which form double helices in all three types of crystalline phases. The splitting of the α-CH$_3$ and OCH$_3$ carbon bands in the crystalline phase of s-PMMA indicates the existence of a double-helix structure also in this case, where it is not possible to distinguish between single and double helices from X-ray diffraction data.[6] The finding that, in the case of the s-PMMA gel in toluene, where s-PMMA predominantly exists in the aggregated state, the aggregated fraction escapes detection in ^{13}C MAS NMR spectra with strong proton decoupling confirms our previous suggestion that the motion of the aggregated segments is slower by about 2 orders of magnitude

(correlation frequency, 10^6–10^7 Hz) than that for s-PMMA in CDCl$_3$ where aggregation does not occur.

For all studied solid samples, including the partially crystalline ones, always only one value of the proton spin-lattice relaxation time in the rotating frame $T_{1\rho}{}^H$ was observed, evidently in consequence of the relatively small size of the crystalline domains (5–9 nm). Numerical $T_{1\rho}{}^H$ values indicate considerably higher segmental mobility in amorphous i-PMMA as compared to the other studied samples. With stereocomplex PMMA, the same value of $T_{1\rho}{}^H$ was observed for protons in i- and s-chains, in agreement with the double-helical structure of the stereocomplex.

References and Notes

(1) Spěváček, J.; Schneider, B. *Adv. Colloid Interface Sci.* **1987**, 27, 81.
(2) Miyamoto, T.; Inagaki, H. *Polym. J.* **1970**, 1, 46.
(3) Könnecke, K.; Rehage, G. *Colloid Polym. Sci.* **1981**, 259, 1062.
(4) Spěváček, J.; Schneider, B.; Baldrian, J.; Dybal, J.; Štokr, J. *Polym. Bull.* **1983**, 9, 495.
(5) Spěváček, J.; Schneider, B.; Dybal, J.; Štokr, J.; Baldrian, J.; Pelzbauer, Z. *J. Polym. Sci., Polym. Phys. Ed.* **1984**, 22, 617.
(6) Kusuyama, H.; Takase, M.; Higashita, Y.; Tseng, H. T.; Chatani, Y.; Tadokoro, H. *Polymer* **1982**, 23, 1256.
(7) Kusuyama, H.; Miyamoto, N.; Chatani, Y.; Tadokoro, H. *Polym. Commun.* **1983**, 24, 119.
(8) de Boer, A.; van Ekenstein, A.; Challa, G. *Polymer* **1975**, 16, 930.
(9) Berghmans, H. Private communication.
(10) Kusanagi, H.; Tadokoro, H.; Chatani, Y. *Macromolecules* **1976**, 9, 531.
(11) Bosscher, F.; ten Brinke, G.; Eshuis, A.; Challa, G. *Macromolecules* **1982**, 15, 1364.
(12) Bosscher, F.; ten Brinke, G.; Challa, G. *Macromolecules* **1982**, 15, 1442.
(13) Spěváček, J.; Schneider, B. *Colloid Polym. Sci.* **1980**, 258, 621.
(14) Spěváček, J.; Schneider, B.; Dybal, J.; Štokr, J. *Croat. Chem. Acta* **1987**, 60, 11.
(15) Dybal, J.; Spěváček, J.; Schneider, B. *J. Polym. Sci., Part B: Polym. Phys.* **1986**, 24, 657.
(16) Spěváček, J.; Schneider, B.; Štokr, J.; Vlček, P. *Makromol. Chem.* **1988**, 189, 951.
(17) Dybal, J.; Spěváček, J. *Makromol. Chem.* **1988**, 189, 2099.
(18) Sundararajan, P. R.; Flory, P. J. *J. Am. Chem. Soc.* **1974**, 96, 5025.
(19) Sundararajan, P. R. *J. Polym. Sci., Polym. Lett. Ed.* **1977**, 15, 699.
(20) Vacatello, M.; Flory, P. J. *Polym. Commun.* **1984**, 25, 258.
(21) Fyfe, C. A. *Solid State NMR for Chemists*; CFC Press: Guelph, Canada, 1983; Chapter 7.
(22) *High Resolution NMR Spectroscopy of Synthetic Polymers in Bulk*; Komoroski, R. A., Ed.; VCH Publishers: Deerfield Beach, FL, 1986; Chapter 4–6.
(23) Voelkel, R. *Angew. Chem., Int. Ed. Engl.* **1988**, 27, 1468.
(24) Schaefer, J.; Stejskal, E. O.; Buchdahl, R. *Macromolecules* **1975**, 8, 291; **1977**, 10, 384.
(25) Edzes, H. T.; Veeman, W. S. *Polym. Bull.* **1981**, 5, 255.
(26) Opella, S. J.; Frey, M. H. *J. Am. Chem. Soc.* **1979**, 101, 5854.
(27) Alemany, L. B.; Grant, D. M.; Pugmire, R. J.; Alger, T. D.; Zilm, K. W. *J. Am. Chem. Soc.* **1983**, 105, 2133.
(28) Spěváček, J. *J. Mol. Struct.* **1985**, 129, 175.
(29) Breitmaier, E.; Voelter, W. *^{13}C NMR Spectroscopy*; Verlag Chemie: Weinheim, FRG, 1974; Chapter 4.
(30) Ault, A.; Ault, M. R. *A Handy and Systematic Catalog of NMR Spectra*; University Science Books: Mill Valley, CA, 1980.
(31) Spěváček, J.; Schneider, B. *Makromol. Chem.* **1974**, 175, 2939.
(32) Katime, I. A.; Quintana, J. R. *Makromol. Chem.* **1988**, 189, 1373.
(33) Vorenkamp, E. J.; Bosscher, F.; Challa, G. *Polymer* **1978**, 20, 59.
(34) Spěváček, J.; Schneider, B. *Polym. Bull.* **1980**, 2, 227.
(35) Laupretre, F.; Monnerie, L.; Virlet, J. *Macromolecules* **1984**, 17, 1397.
(36) Jo, Y. S.; Maruyama, Y.; Inoue, Y.; Chujo, R.; Tasaka, S.; Miyata, S. *Polym. J.* **1987**, 19, 769.
(37) Mitchell, G. R.; Windle, A. H. *Colloid Polym. Sci.* **1982**, 260, 754.

(38) Birshtein, T. M.; Merkuryeva, A. A.; Goryunov, A. N. *Vysoko-mol. Soedin., Ser. A* **1983**, *25*, 124.

(39) Tanaka, H.; Gomez, M. A.; Tonelli, A. E. *Macromolecules* **1988**, *21*, 2934.

(40) Yoon, D. Y.; Flory, P. J. *Polymer* **1975**, *16*, 645.

(41) Lovell, R. A.; Windle, A. H. *Polymer* **1981**, *22*, 175.

(42) Cheung, T. T. P.; Gernstein, B. C.; Ryan, L. M.; Taylor, R. E.; Dybowski, D. R. *J. Chem. Phys.* **1980**, *73*, 6059.

(43) Johnson, J. F.; Porter, R. S. In *The Stereochemistry of Macromolecules*; Ketley, A. D., Ed.; Marcel Dekker: New York, 1968; Vol. 3, Chapter 5.

(44) Spěváček, J.; Schneider, B. *Polymer* **1978**, *19*, 63.

High-Resolution Carbon-13 Nuclear Magnetic Resonance of Trigonal and Orthorhombic Crystals of Poly(oxymethylene)

Masamichi Kobayashi*

Department of Macromolecular Science, Faculty of Science, Osaka University, Toyonaka, Osaka 560, Japan

Masao Murano and Atsushi Kaji

Katata Research Center, Toyobo Co. Ltd., Katata, Otsu, Shiga 520-02, Japan

Received September 12, 1989

ABSTRACT: ^{13}C NMR spectra of a needlelike single crystal of trigonal poly(oxymethylene) (t-POM) have been investigated in comparison with those of ordinary semicrystalline samples of t-POM. The ^{13}C signal in the single crystal splits into a doublet at 88.5 and 87.7 ppm in contrast to the singlet at 88.4 ppm in the semicrystalline samples. The split pattern is ascribed to the inequivalent monomeric units in the crystal field of the t-POM lattice. The corresponding ^{13}C signal of a plate-shaped single crystal of orthorhombic POM (o-POM) appears at 82.0 ppm as a singlet as anticipated from the space group of o-POM. The large chemical shift difference (6 ppm) between t-POM and o-POM was interpreted in terms of the intramolecular γ-gauche shielding and the intermolecular packing effect.

Introduction

Since the pioneering works of Schaefer and Stejskal[1–3] in the field of solid-state, high-resolution ^{13}C NMR spectroscopy of polymers, application of this method to the structural studies of crystalline polymers is rapidly increasing.

The present study is concerned with fine structure in the high-resolution ^{13}C NMR spectra due to the inequivalent carbon atoms in the trigonal phase of poly(oxymethylene) and the difference in the isotropic ^{13}C chemical shift between the trigonal and orthorhombic phases. Poly(oxymethylene) (abbreviated as POM) is one of the typical crystalline linear polymers having a simple chemical structure $(CH_2O)_n$. There are two crystal modifications: the trigonal (t-POM) and orthorhombic (o-POM) forms. The trigonal form is stable at ambient conditions and is obtained exclusively through the ordinary crystallization procedures from the melt and dilute solutions. The orthorhombic form is metastable at ambient conditions and transforms to the trigonal form by heating above 69 °C.[4,5] The o-POM samples are obtained by some specific polymerization processes.[6–8]

The high-resolution ^{13}C NMR spectrum (measured at 45 MHz) of t-POM has been studied first by Veeman et al.[9] by means of the proton-decoupled magic-angle-spinning (MAS) technique with and without cross-polarization (CP). They demonstrated that the t-POM sample (a Delrin resin of E. I. du Pont de Nemours and Co., Inc.) gave rise to a singlet signal at about 90 ppm (measured from TMS) with a line width of 3.7–5.7 ppm depending on the MAS frequency. The measurement of T_1 and $T_{1\rho}$ of ^{13}C indicated the coexistence of two phases: a crystalline phase having short $T_{1\rho}$ and long T_1 and an amorphous phase with a longer $T_{1\rho}$ and a shorter T_1. Cholli et al.[10] measured ^{13}C CP-MAS NMR spectra (measured at 37.7 MHz) of a semicrystalline t-POM sample. Although the ^{13}C signal was not resolved into the crystalline and amorphous components, the amorphous ^{13}C resonance was isolated from the crystalline one by the aid of difference in relaxation behavior (by means of a modified CP-MAS technique). They concluded that the amorphous ^{13}C peak appeared at about 1 ppm downfield compared to the crystalline peak. Kurosu et al.[11] measured the ^{13}C CP-MAS NMR spectra (measured at 67.8 MHz) of t-POM on various samples obtained from a commercial resin (Tenac 7010 of Asahi Chem. Ind. Co., Ltd.) treated by different crystallization procedures. They observed a singlet signal centered at 88.5 ppm. The observed band profile was simulated by two Lorentzian functions centered at 88.5 and 89.4–91.5 ppm (depending on the crystallinity of the samples), the former and the latter being ascribed to the crystalline and amorphous phases, respectively. They also measured the powder pattern spectra of the same samples and derived the values of the elements of the chemical shift tensors of the crystalline and amorphous phases. Thereafter, Kurosu et al.[12] measured ^{13}C CP-MAS and powder pattern spectra of a POM sample which contained a small amount of o-POM, the major component being t-POM, and evaluated the isotropic ^{13}C chemical shift of o-POM.

Thus, in the previous papers, the carbon atoms in the